Two-Phase Flow Pressure Drop in Superhydrophobic Channels

Kimberly A. Stevens, Julie Crockett, Daniel R. Maynes, Brian D. Iverson
Department of Mechanical Engineering
Brigham Young University
Provo, UT USA

Superhydrophobic surfaces promote dropwise condensation, which increases the rate of thermal transport, making them desirable for use in condensers. Adiabatic two-phase flow loops have been constructed to gain insight into the hydrodynamics of two-phase systems, laying the groundwork for further study of condensing flow on superhydrophobic surfaces. A two-phase flow loop to measure pressure drop and visualize the flow patterns of two-phase flow in superhydrophobic channels relative to classical hydrophilic and hydrophobic surfaces was built and validated. Good agreement was found between observed pressure drops and theoretical and experimental correlations in the literature. The percent reduction (relative to a classical channel) in two-phase pressure drop for a channel with with a single superhydrophobic wall is approximately the same percent reduction in pressure drop experienced by a single-phase flow.

1 Introduction

Superhydrophobic surfaces have recently gained much media and scholarly attention due to their drag-reducing, self-cleaning, and ice-preventing properties. One particularly promising application for superhydrophobic surfaces is in condensation. It has been shown that condensation on superhydrophobic surfaces promotes drop-wise condensation, which is known to increase heat transfer around 5-7 times [1,2] relative to film-wise condensation. Increased heat transfer rates would benefit a number of applications such as desalination, energy conversion [3], atmospheric water harvesting [4,5], and other high heat flux applications [6] involving condensation. However, very little work has been done with condensation on superhydrophobic surfaces in a flow environment. The objective of this work is to explore the parameters which influence heat transfer for condensing flow in a superhydrophobic channel, beginning by investigating the hydrodynamics in an adiabatic two-phase channel flow. This paper specifically addresses how the driving pressure in a superhydrophobic channel changes relative to classical channels.

2 Background

2.1 Superhydrophobic Surfaces

A superhydrophobic surface has a solid-liquid contact angle (CA) greater than 150° [7], as shown in Figure 1, and contact angle hysteresis less than 10°.

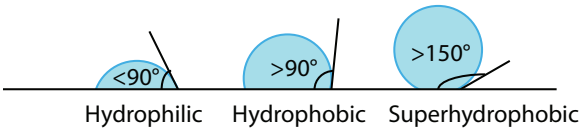

Fig. 1. The solid-liquid contact angle determines the hydrophobicity of a surface. Hydrophilic surfaces have a contact angle less than 90°, while hydrophobic surfaces have contact angles greater than 90°. Superhydrophobic surfaces have a solid-liquid contact angle of greater than 150°.

Superhydrophobic surfaces are created by adding micro- or nano-structured features and then changing the surface chemistry to be hydrophobic. This is commonly accomplished by adding a hydrophobic coating. When a static droplet is sitting on top of a superhydrophobic surface, surface tension can prevent the liquid from penetrating into the cavities, creating a layer of air between the solid and liquid surfaces, as shown in Figure 2. In this case, the droplet is said to be in a non-wetting, or Cassie state. If the pressure in the liquid is too high, it will overcome the surface tension and liquid will enter the cavities; the droplet is then said to be in a wetting, or Wenzel state. The threshold for the pressure required for the liquid to wet a superhydrophobic surface is traditionally given by the Laplace pressure, given by the Young-Laplace Equation:

$$\Delta P = P_{water} - P_{air} = \gamma\left(\frac{1}{R_1} + \frac{1}{R_2}\right) \quad (1)$$

where γ is the surface tension, R_1 and R_2 are the surface radii

of curvature. For superhydrophobic microribs, this becomes

$$\Delta P = -\frac{2\gamma cos(\theta)}{w_c} \tag{2}$$

where θ is the contact angle for a droplet on a smooth surface of equivalent surface chemistry, and w_c is the width of the cavity between the ribs.

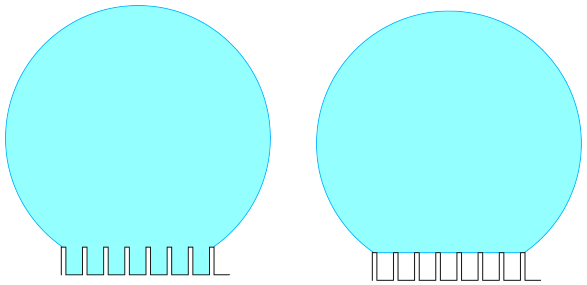

Fig. 2. When in a Wenzel sate, the liquid fills the spaces between the cavities, as shown on left. When in a non-wetting, or Cassie state, the liquid only touches the solid at a fraction of the surface, as shown on right.

2.2 Adiabatic Two-Phase Flow

Adiabatic two-phase flows composed of a liquid and gas are commonly studied to gain insight into condensing and boiling flows. In adiabatic flows, the vapor fraction and flow regime do not change along the length of the channel, thereby isolating the hydrodynamic phenomena (i.e. pressure drop and flow regime behavior). Liquid and gas flows of a set rate are mixed together and observed in a channel. In this manner, the pressure drop, vapor fraction, and flow regime are fixed.

Early work by Lockhart and Martinelli [8] and Chisholm and Laird [9, 10] laid the foundation for predicting pressure drop for two-phase flow in channels. In their work, the two-phase pressure drop is expressed in terms of a two-phase multiplier, ϕ^2, which is the two-phase pressure gradient normalized by the single-phase pressure gradient that would result if the liquid (denoted by subscript L) or gas (G) component of the two-phase flow flowed alone through the channel:

$$\phi_L^2 = (\frac{dp}{dz}F)_{TP}/(\frac{dp}{dz}F)_L \tag{3}$$

$$\phi_G^2 = (\frac{dp}{dz}F)_{TP}/(\frac{dp}{dz}F)_G \tag{4}$$

where the F denotes that the frictional component of the pressure gradient, as opposed to that associated with a phase change or gravity. The multipliers are often correlated in terms of the Martinelli parameter, χ:

$$\chi = [(\frac{dp}{dz}F)_L/(\frac{dp}{dz}F)_G]^{1/2} \tag{5}$$

In practice, χ reduces to:

$$\chi = \frac{\dot{m}_l}{\dot{m}_g}\sqrt{\frac{\rho_g}{\rho_l}} = \sqrt{\frac{\mu_l \dot{V}_l}{\mu_g \dot{V}_g}} \tag{6}$$

Chisholm and Laird [9] found that the two-phase multipliers could be roughly correlated with the Martinelli parameter with the following relations:

$$\phi_L^2 = 1 + \frac{C}{\chi} + \frac{1}{\chi^2} \tag{7}$$

$$\phi_G^2 = 1 + C\chi + \chi^2 \tag{8}$$

where C is a constant dependent on the flow regime of the liquid and gas phases. Though it is known that these correlations deviate significantly from reality for many flow conditions, they are the basis for much of the two-phase flow work that followed. Dozens of correlations exist for predicting two-phase flow for a variety of channel geometries and orientations, working fluids, and velocities. Sun and Mishima [11] and Asadi et al. [12] have provided excellent reviews specifically for mini- and micro-channel flow. Kim and Mudawar developed a universal correlation for a wide range of fluids, flow rates, and channel shapes, constructed from over 7000 data points compiled from over 36 studies [13, 14]. However, with all the work that has been done for pressure drop in two-phase flow, there has been limited discussion of the effect of surface wettability, and even less exploration of the effect of superhydrophobic surfaces specifically.

2.2.1 Wettability and Two-Phase Flow

It is recognized that changing the contact angle has an influence on the transition between the many flow regimes that occur in two-phase flow [15, 16]. Huh et al. [17] observed more flow regimes for hydrophobic than hydrophilic microchannels. Barajas and Panton [18] found considerably different flow maps for hydrophilic relative to hydrophobic tubes. Serizawa et al. [19] found that the influence of surface wettability impacts the flow regime at the interface of the channel surface and fluid and concluded that the impact would be higher for smaller (in the mini and micro-range) channels. While it is clear that wettability influences the flow regime, there is wide disagreement between studies on the effect of wetability on pressure drop.

Takamasa et al. [20] found the effect of wettability to be insignificant on the pressure drop in 20 mm diameter tubes. Phan et al. [21] investigated flow boiling in a 0.5 x 5 mm rectangular channel with surface contact angles of 26, 49, 63 and 103, with mass fluxes of 100 and 120 $\frac{kg}{m^2 s}$, and a vapor quality range of 0.01-0.06. They found that a higher contact angle leads to higher pressure drop. Cho and Wang [15] observed differences in pressure drop for three surfaces of varying wettability (CA=80°, 103°, and 124°). The surface with the highest contact angle had a significantly higher pressure drop, but it was also much rougher than the other surfaces. There was no conclusive difference in pressure drop

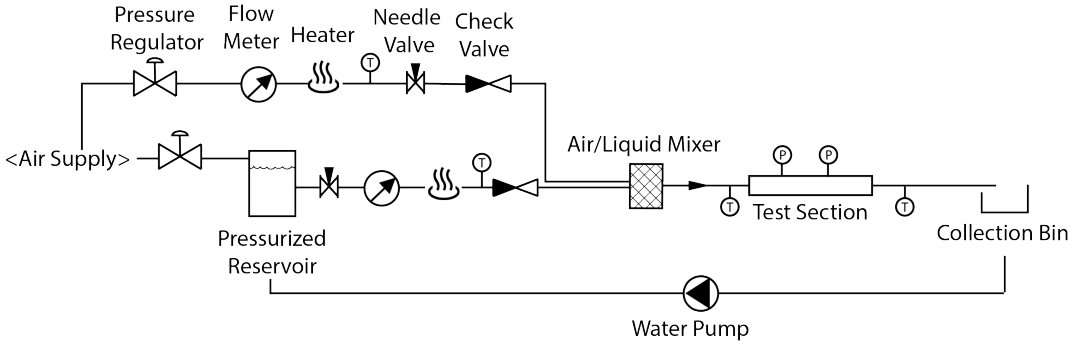

Fig. 3. Schematic of the two-phase flow loop.

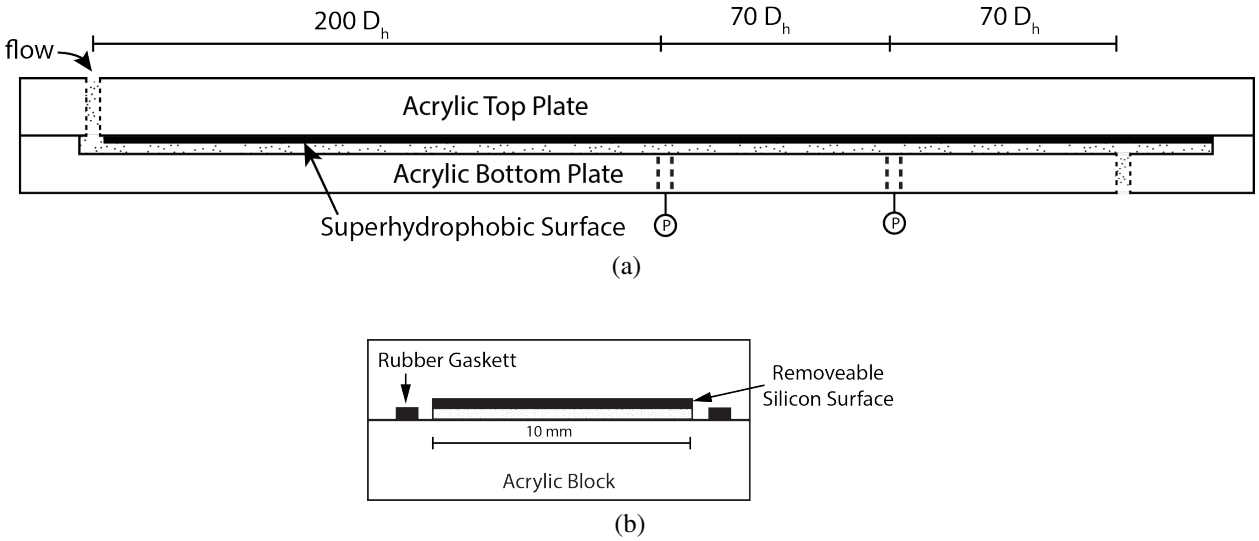

Fig. 4. The test section (a) has a hydraulic diameter of about 700 μm, a height of 300 μm, and a width to height ratio of 30. A cross-sectional view of the channel is shown in (b).

for the other two surfaces. Choi et al. [22] measured flow in a 530 x 499 μm channel with all channel sides exhibiting CA of 25°and 105°. The liquid and air superficial velocities ranged from 0.25-0.43 m/s and 4.5-40 m/s, respectively. They found that the hydrophobic channel had a smaller pressure drop, and pointed out that the fluid was also in a different flow regime. Wang et al. [23] observed a decrease in pressure drop for two-phase flow in a square channel (4 mm x 4 mm) with a superhydrophobic surface created from randomly distributed silica particles coated with PDMS (CA=155°). In summary, there is not good agreement in the literature on the effect of wettability on two-phase pressure drop; it likely depends on the range of flow rates and channel size tested. With the exception of Wang [23], very high vapor fraction flows, common to PEM fuel cells, the influence of a superhydrophobic wall on two-phase pressure drop has not been explored. Data for a wider range of vapor fractions is necessary to understand how superhydrophobic surfaces influence two-phase pressure drop in a wider range of applications.

3 Methods

An adiabatic flow loop was designed and constructed to measure and observe two-phase channel flow, as shown in Figure 3. Air and water streams of a fixed flow rate were mixed together, and the two-phase mixture was observed as it flowed through the test section. Air was used to pressurize a tank containing deionized water. Pressure regulators were used to set the pressure in a line containing house air. The air and water flow rates were controlled with needle valves and pressure regulators and were measured with in-line flow meters (Omega FLR1004-D, 200-1000 mL/min and Omega FLR1007, 13-100 mL/min). The air and water flows were mixed a $\frac{1}{16}$ inch T-shaped junction before entering a rectangular test section, as shown in Figure 4a. The flow was allowed to develop for 200 hydraulic diameters before the differential pressure was measured across the test section (70 hydraulic diameters) (Omega PX409-2.5DWU5V). The taps leading to the pressure transducer were filled with water, and were located on the bottom of the channel to prevent air bubbles from entering the taps. The flow then exited the test section to atmosphere after an additional 70 hydraulic diam-

eters. Temperature was measured with T-type thermocouples before and after the test section. Flow rate, pressure, and temperature were recorded at 200 hz. The pressure signal was filtered with a Butterworth filter at 45 hz to remove electrical noise. During testing, for each flow rate the flow was allowed to reach steady state and the flow rates, pressure, and temperature were time-averaged over a period of at least 30 seconds, a sufficiently long period of time for the fluctuations in the flow to not influence the mean signal. Three sides of the test section were made of clear acrylic to allow visual access, and the remaining side was a removable silicon surface that was either superhydrophobic or hydrophilic, as shown in Figure 4b. The removable surface was held in place with a strip of double-sided tape that ran along the length of the surface. The height of the channel was measured with a depth micrometer, which has an accuracy of +/- 0.00025 inches. The acrylic channel was precision machined to be perfectly flat, and the channel was held together with two steel plates that ran the length of the channel in order to prevent any deflection caused by the rubber gasket seal. Toggle and C-clamps were used to hold the two sides of the channel together and were tightened until the differential pressure measurement stopped changing. The hydraulic diameter of the test section was 700 μm, with a height of 300 μm, and a width to height ratio of 30. With such a high aspect ratio, the channel approached a parallel plate scenario, though the differences are not negligible.

The superhydrophobic surfaces were manufactured using standard photolithography and a deep reactive ion etch, then coated with thin layer of Teflon, as described in [24]. The structure was ribs with a cavity fraction (ratio of the area between the ribs to the total area) of 80%. The ribs were 15-20 microns in height, as shown in Figure 5. These surfaces have a contact angle of 150°. The control, or hydrophilic, surfaces were smooth silicon wafers with no coating, and have a contact angle of 30°.

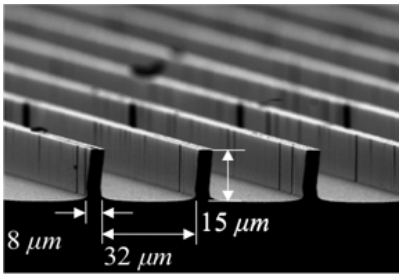

Fig. 5. Scanning Electron Microscope image of a superhydrophobic surface.

3.1 Validation

In order to validate the channel setup, single phase pressured drop measurements were compared with those predicted in the literature. Differential pressure measurements for single-phase flow were taken in the channel with hydrophilic and superhydrophobic surfaces. The Poiseuille number in a hydrophilic, or classical, rectangular channel was predicted with a correlation developed by Shah and London [25],

$$f \cdot Re = 24(1 - 1.3553\eta + 1.9467\eta^2 - 1.7012\eta^3 + 0.9564\eta^4 - 0.2537\eta^5), \quad (9)$$

where η is the aspect ratio of the channel, H/W. The pressure drop for parallel plate flow with one superhydrophobic surface was predicted using relations developed by Philip [26] and Enright et al. [27]. These relations for asymmetric parallel plate flow predict a 9% reduction in Poiseuille number. It was assumed that a rectangular channel with a high aspect ratio would experience a similar reduction, which was validated numerically. The predicted and measured Poiseuille numbers for the classical and superhydrophobic channels are shown in Figure 6. The superhydrophobic channel experienced an average decrease in pressure drop of 10%, only slightly higher than the predicted 9%, and within the experimental uncertainty.

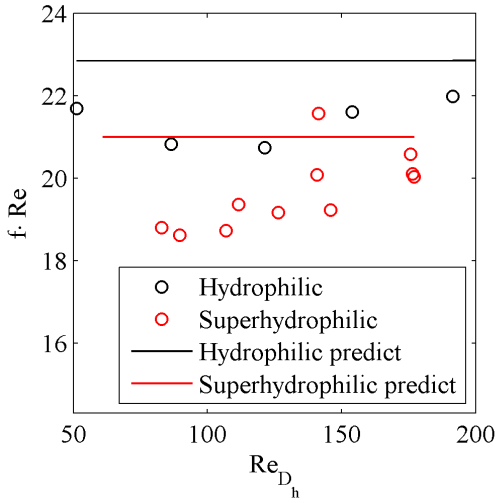

Fig. 6. Poiseuille number for single-phase channel flow. The frictional factor used is the Fanning friction factor. HL predict is the predicted number for a hydrophilic, or classical channel. SH predict is the number predicted for a channel with one superhydrophobic surface.

In order to validate the two-phase flow setup, the two-phase frictional multiplier predicted by the correlation from Kim and Mudawar [13] was compared with the two-phase frictional multiplier measured in the channel. The single-phase liquid flow pressure gradient used in the correlation was predicted using Equation 9, given by Shah and London [25]. The comparison is plotted in Figure 7 and is for a range of flow rates corresponding to liquid only Reynolds

numbers of 50-200 and gas only Reynolds numbers of 20-215. The agreement between the prediction and measured value is better than 20%, which is reasonable given that the correlation was only accurate to 30%. The good agreement for both the single- and two-phase pressure drop measurements with the literature allow for reasonable confidence in the following results.

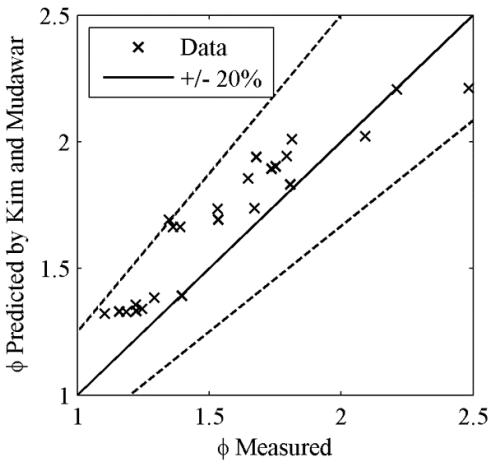

Fig. 7. Two-phase frictional multiplier predicted by Kim and Mudawar [13] compared with measured. The data shown here corresponds to a liquid only Reynolds number 50-200 and a gas only Reynolds number of 20-215.

4 Results and Conclusion

The ratio between the two-phase frictional multiplier for a superhydrophobic surface and a classical surface,

$$\phi\ ratio: \frac{\phi_{superhydrophobic}}{\phi_{hydrophobic}}, \tag{10}$$

is shown in Figure 8. Each point shown is the average of three separate measurements. The superhydrophobic boundary reduces the two-phase frictional multiplier by an average of 13% for the range of flow rates tested. Such a reduction is reasonable since a reduction of around 10% was predicted and measured for an identical single-phase flow scenario. Future work will include exploration of the effect of varying the cavity fraction on the reduction in pressure drop, but for an 80% cavity fraction superhydrophobic wall, for the range of flow rates explored, the single-phase and two-phase reduction in pressure drop are of similar magnitude. This result can be used to predict the frictional pressure drop in flow condensing channels with superhydrophobic walls.

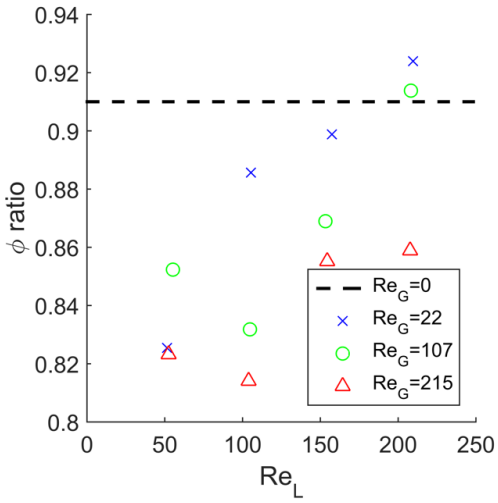

Fig. 8. The ratio between the two-phase frictional multiplier for a superhydrophobic surface and a classical surface.

References

[1] Rose, J. W., 2002. "Dropwise condensation theory and experiment: a review". *Proceedings of the Institution of Mechanical Engineers Part a-Journal of Power and Energy,* **216**(A2), pp. 115–128.

[2] Lienhard-IV, J., and Lienhard-V, J., 2003. *A Heat Transfer Textbook*, 3rd ed. Pologiston, Cambridge.

[3] Glicksman, L. R., and Hunt, A. W., 1972. "Numerical simulation of dropwise condensation". *International Journal of Heat and Mass Transfer,* **15**(11), p. pp. 22512269.

[4] Love, J. C., Estroff, L. A., Kriebel, J. K., Nuzzo, R. G., and Whitesides, G. M., 2005. "Self-assembled monolayers of thiolates on metals as a form of nanotechnology". *Chemical Reviews,* **105**(4), pp. 1103–69.

[5] Andrews, H. G., Eccles, E. A., Schofield, W. C., and Badyal, J. P., 2011. "Three-dimensional hierarchical structures for fog harvesting". *Langmuir,* **27**(7), pp. 3798–802.

[6] Leach, R. N., Stevens, F., Langford, S. C., and Dickinson, J. T., 2006. "Dropwise condensation: experiments and simulations of nucleation and growth of water drops in a cooling system". *Langmuir,* **22**(21), pp. 8864–72.

[7] Law, K.-Y., 2014. "Definitions for hydrophilicity, hydrophobicity, and superhydrophobicity: Getting the basics right". *Journal of Physical Chemistry Letters,* **5**, p. 686688.

[8] Lockhart, R., and Martinelli, R., 1949. "Proposed correlation of data for isothermal two-phase, two-component flow in pipes". *Chemical Engineering Progress,* **45**(1), pp. 39–48.

[9] Chisholm, D., and Laird, A., 1958. "Two-phase flow in rough tubes". *Trans. ASME,* **80**(2), pp. 276–286.

[10] Chisholm, D., 1967. "A theoretical basis for lockhart-martinelli correlation for 2-phase flow". *International*

Journal of Heat and Mass Transfer, **10**(12).

[11] Sun, L., and Mishima, K., 2009. "Evaluation analysis of prediction methods for two-phase flow pressure drop in mini-channels". *International Journal of Multiphase Flow,* **35**(1), pp. 47–54.

[12] Asadi, M., Xie, G., and Sunden, B., 2014. "A review of heat transfer and pressure drop characteristics of single and two-phase microchannels". *International Journal of Heat and Mass Transfer,* **79**, pp. 34–53.

[13] Kim, S. M., and Mudawar, I., 2012. "Universal approach to predicting two-phase frictional pressure drop for adiabatic and condensing mini/micro-channel flows". *International Journal of Heat and Mass Transfer,* **55**(11-12), pp. 3246–3261.

[14] Kim, S.-M., and Mudawar, I., 2014. "Review of databases and predictive methods for pressure drop in adiabatic, condensing and boiling mini/micro-channel flows". *International Journal of Heat and Mass Transfer,* **77**, pp. 74–97.

[15] Cho, S. C., and Wang, Y., 2014. "Two-phase flow dynamics in a micro channel with heterogeneous surfaces". *International Journal of Heat and Mass Transfer,* **71**, pp. 349–360.

[16] Cubaud, T., Ulmanella, U., and Ho, C.-M., 2006. "Two-phase flow in microchannels with surface modifications". *Fluid Dynamics Research,* **38**(11), pp. 772–786.

[17] Huh, D., Kuo, C. H., Grotberg, J. B., and Takayama, S., 2009. "Gasliquid two-phase flow patterns in rectangular polymeric microchannels: effect of surface wetting properties". *New journal of physics,* **11**, p. 75034.

[18] Barajas, A. M., and Panton, R. L., 1993. "The effects of contact-angle on 2-phase flow in capillary tubes". *International Journal of Multiphase Flow,* **19**(2), pp. 337–346.

[19] Serizawa, A., Feng, Z. P., and Kawara, Z., 2002. "Two-phase flow in microchannels". *Experimental Thermal and Fluid Science,* **26**(6-7), pp. 703–714.

[20] Takamasa, T., Hazuku, T., and Hibiki, T., 2008. "Experimental study of gasliquid two-phase flow affected by wall surface wettability". *International Journal of Heat and Fluid Flow,* **29**(6), pp. 1593–1602.

[21] Phan, H. T., Caney, N., Marty, P., Colasson, S., and Gavillet, J., 2011. "Flow boiling of water in a minichannel: The effects of surface wettability on two-phase pressure drop". *Applied Thermal Engineering,* **31**(11-12), pp. 1894–1905.

[22] Choi, C., Yu, D. I., and Kim, M., 2011. "Surface wettability effect on flow pattern and pressure drop in adiabatic two-phase flows in rectangular microchannels with t-junction mixer". *Experimental Thermal and Fluid Science,* **35**(6), pp. 1086–1096.

[23] Wang, Y., Al Shakhshir, S., Li, X., and Chen, P., 2012. "Superhydrophobic flow channel surface and its impact on pem fuel cell performance". *International Journal of Low-Carbon Technologies*.

[24] Prince, J., 2013. "The influence of superhydrophobicity on laminar jet impingement and turbulent flow in a channel with walls exhibiting riblets". Dissertation.

[25] Shah, R. K., and London, A. L., 1978. *Laminar Flow Forced Convection in Ducts*. Academic Press.

[26] Philip, J. R., 1972. "Flows satisfying mixed no-slip and no-shear conditions". *Zeitschrift Fur Angewandte Mathematik Und Physik,* **23**(3), pp. 353–372.

[27] Enright, R., Hodes, M., Salamon, T., and Muzychka, Y., 2014. "Isoflux nusselt number and slip length formulae for superhydrophobic microchannels". *Journal of Heat Transfer,* **136**(1).